THE JOURNAL OF COMPARATIVE NEUROLOGY 500:255–266 (2007)

Callosal Axon Arbors in the Limb Representations of the Somatosensory Cortex (SI) in the Agouti (*Dasyprocta primnolopha*)

E.G. ROCHA,[1] L.F. SANTIAGO,[1] M.A.M. FREIRE,[1] W. GOMES-LEAL,[1] I.A. DIAS,[1] R. LENT,[2] J.C. HOUZEL,[2] J.G. FRANCA,[3] A. PEREIRA JR.,[1] AND C.W. PICANÇO-DINIZ[1]*

[1]Laboratório de Neuroanatomia Funcional, Departamento de Morfologia–Universidade Federal do Pará, 66075-900 Belém, PA, Brasil

[2]Departamento de Anatomia, Instituto de Ciências Biomédicas. Universidade Federal do Rio de Janeiro, 21949-900 Rio de Janeiro, Brasil

[3]Laboratório de Neurobiologia II, Instituto de Biofísica Carlos Chagas Filho–Universidade Federal do Rio de Janeiro, 21949-900 Rio de Janeiro, RJ, Brasil

ABSTRACT

The present report compares the morphology of callosal axon arbors projecting from and to the hind- or forelimb representations in the primary somatosensory cortex (SI) of the agouti (*Dasyprocta primnolopha*), a large, lisencephlic Brazilian rodent that uses forelimb coordination for feeding. Callosal axons were labeled after single pressure (n = 6) or iontophoretic injections (n = 2) of the neuronal tracer biotinylated dextran amine (BDA, 10 kD), either into the hind- (n = 4) or forelimb (n = 4) representations of SI, as identified by electrophysiological recording. Sixty-nine labeled axon fragments located across all layers of contralateral SI representations of the hindlimb (n = 35) and forelimb (n = 34) were analyzed. Quantitative morphometric features such as densities of branching points and boutons, segments length, branching angles, and terminal field areas were measured. Cluster analysis of these values revealed the existence of two types of axon terminals: Type I (46.4%), less branched and more widespread, and Type II (53.6%), more branched and compact. Both axon types were asymmetrically distributed; Type I axonal fragments being more frequent in hindlimb (71.9%) vs. forelimb (28.13%) representation, while most of Type II axonal arbors were found in the forelimb representation (67.56%). We concluded that the sets of callosal axon connecting fore- and hindlimb regions in SI are morphometrically distinct from each other. As callosal projections in somatosensory and motor cortices seem to be essential for bimanual interaction, we suggest that the morphological specialization of callosal axons in SI of the agouti may be correlated with this particular function. J. Comp. Neurol. 500:255–266, 2007.

Indexing terms: corpus callosum; hindlimb; forelimb; biotinylated dextran amine; agouti

Grant sponsor: CAPES; Grant number: 0024/01-5; Grant sponsor: CNPq; Grant number: 411530/2003-8; Grant sponsor: PRONEX; Grant number: E-26/171.210/2003.

Current address for M.A.M. Freire: International Institute for Neuroscience of Natal (IINN), Rua Professor Francisco Luciano de Oliveira, 2460, 59066-060 Natal, RN, Brasil.

*Correspondence to: Cristovam Wanderley Picanço Diniz, DrSci., Universidade Federal do Pará, Centro de Ciências Biológicas, Campus Universitário do Guama, 66075-900–Belém/Pa, Brasil.
E-mail: cwpdiniz@ufpa.br

Received 24 March 2006; Revised 10 July 2006; Accepted 8 August 2006

DOI 10.1002/cne.21167

Published online in Wiley InterScience (www.interscience.wiley.com).

Somatosensory perception emerges from the encoding of information coming from various peripheral mechanosensory receptors and reaches the central nervous system through distinct parallel channels. These channels connect to several areas and nuclei in a progressive integration at both subcortical and cortical levels through networks of forward and feedback connections (DeFelipe et al., 2002; Douglas and Martin, 2004; Kaas, 2004). At the cortical level, interhemispheric projections provide information necessary to integrate bilateral cortical activation (Cardoso de Oliveira et al., 2001; Houzel et al., 2002; Swinnen, 2002).

At the cellular level the morphological complexity of dendritic and axonal arbors plays crucial roles in the signal transformation through isolated neurons and networks, but, classically, quantitative analysis of neuronal morphology have focused almost entirely on the dendritic tree (Binzegger et al., 2005). In particular, this is the case for the majority of studies dedicated to callosal connections in different species: rat (Hubener and Bolz, 1988), golden hamster (Diao and So, 1991), cat (Voigt et al., 1988; Olavarria, 2001), tree shrew (Pritzel et al., 1988), star-nosed mole (Catania and Kaas, 2001), ferret (Manger et al., 2004), mouse (Porter and White, 1986), as well as in both human and monkey brains (Elston and Rosa, 2000; Jacobs et al., 2001; Soloway et al., 2002).

It is well known that callosal activity is essential for the cortical representation of bilateral integrated motor tasks (Cardoso de Oliveira et al., 2001; Rokni et al., 2003), but current knowledge of the structure of interhemispheric axons is very limited. In order to fill this gap it is relevant to investigate the morphometry and the topology of interhemispheric connections in animals with less complex brains and simpler bimanual manipulation (restricted to the forelimbs, for example) (Kaas, 2004). This is the case of the rodent agouti (*Dasyprocta primnolopha*), which was used as an experimental animal in the present study.

Agouti is the name of a group of burrowing rodents of the genus *Dasyprocta* (Linnaeus, 1776), native to tropical America, possessing a medium-sized body (about 3.5 kg) with diurnal habits and terrestrial habitat, which uses the forelimbs to manipulate food while eating, sitting on their hindlimbs. The agouti has a large lisencephalic brain well suited for mapping studies that poses fewer experimental difficulties than both gyrencephalic species (e.g., primates) and small lisencephalic rodents (e.g., rat).

Moreover, the agouti displays bimanual motor skills that are likely to rely on a higher degree of bilateral cooperation between the forelimbs as compared to the hindlimbs. We hypothesized that the morphology of somatosensory cortex (SI) callosal projections would reflect such differences, thus being instrumental in unraveling the participation of callosal connections in these bilateral behaviors.

In previous studies we demonstrated that terminal arbors from intrinsic axons in the visual cortex of cat and cebus monkeys (Amorim and Picanço-Diniz, 1996a,b; Gomes-Leal et al., 2002) can be differentiated on the basis of their morphometric features, which include density of branch points, boutons, and segments/mm as well as average segment length. Reasoning that the same might apply to agouti SI callosal axons, we compared the morphological features of axon samples from two different regions of the somatosensory topographic map (hind- and forelimbs), with an aim at detecting differences that could be related to behavior. Computer-assisted reconstruction of callosal axon fragments was performed following a previously established protocol (Amorim and Picanço-Diniz, 1996a; Gomes-Leal et al., 2002), as was the analysis of morphometric parameters such as segment length, branching points, and densities of branching points, segments, and boutons ("en passant" and "terminaux"). Following Binzegger et al. (2005), we expected that the investigation of similar and/or different features of callosal axonal fragments would contribute to current debate regarding diversity versus stereotypy of cortical neurons (DeFelipe et al., 2002; Douglas and Martin, 2004; Migliore and Shepherd, 2005).

Our results show that axon terminals of SI callosal fibers to the hind- and forelimb representations of the agouti display distinct morphometric properties that may be related to object manipulation by forelimbs, as opposed to postural and locomotion movements by hindlimbs. These findings reveal the existence of morphologically distinct channels of interhemispheric connections at the level of primary sensory area in rodent cortex.

MATERIALS AND METHODS

Surgical procedures, electrophysiological recording, and tracer injection

Eight animals received a single injection of the anterograde tracer biotinylated dextran amine (10 kD) into the left SI representation of the forelimb (n = 4), or of the hindlimb (n = 4), as assessed by intracortical multiunit recordings. All experimental procedures followed the *Principles of Laboratory Animal Care* (NIH publication No 86-23, revised 1985), as well as the *Local Ethics Committee on Experimental Animal Research* of the Federal University of Pará, Brazil. Eight male adult agoutis weight 2.7–3.2 kg were used in the present investigation. Animals were donated by Emilio Goeldi Zoo-Botanic Museum, under license of the Brazilian Institute of the Environment and Renewable Natural Resources (IBAMA, 207419-0030/2003) and maintained in the animal facility of Federal University of Pará. One day before the recording session the animal was premedicated with dexamethasone (Decadron, Prodome, 1.0 mg/kg, intramuscular (i.m.)) to prevent brain edema and vitamin K (Kanakion, Roche, 1.0 mg/kg, i.m.) to avoid excessive bleeding. On the following day, anesthesia was induced by i.m. injection of a mixture of ketamine (10 mg/kg) and xylazine (1 mg/kg). Anesthesia level was monitored by testing corneal reflex and supplementary doses were administered as needed. Body temperature was maintained at about 37°C. All efforts were made in order to use as few animals as possible and to minimize unnecessary animal discomfort, distress, and pain.

The head of the animal was secured with ear and mouth pieces into a standard headholder (David Kopf, Germany) and a craniotomy was performed to expose part of the left SI region. A varnish-insulated tungsten microelectrodes (1 M° at 1 kHz; FHC, Bowdoinham, ME) positioned with a micromanipulator was used to explore cortical multiunit activity (David Kopf). The multiunit signal was differentially amplified, bandpass-filtered between 1 and 3 kHz (ME04011, FHC), and fed simultaneously to a dual-beam storage oscilloscope (1476A, BK Precision, Yorba Linda, CA) and an audio monitor (SR771, Sansui, Japan). Me-

TABLE 1. Summary of the Experimental Cases and Labeling

Subject	Delivering procedure/ histochemical reaction	Injection site	Sectioning plane	Contralateral projection
Cc 02	Iontophoresis/BDA	SI (HL)–LH	LH-tangential	
			RH-coronal	SI (HL), SII
Cc 03	Pressure/BDA	SI (FL)–LH	Tangential	SI (FL, F), SII (FL)
Cc 04	Iontophoresis/BDA	SI (FL)–LH	LH-tangential	
			RH-coronal	SI (FL), SII (FL)
Cc 12	Pressure/BDA	SI (FL)–LH	Tangential	SI (FL, F), SII (FL)
Cc 10	Pressure/BDA + CO	SI (FL)–LH	Tangential	SI (FL, F, IL), SII (FL), PR
Cc 11	Pressure BDA	SI (HL)–LH	Tangential	SI (HL), SII (HL)
Cc 16	Pressure/BDA	SI (HL)–LH	Tangential	SI (HL), SII (HL)
Cc 17	Pressure/BDA + CO	SI (HL)–LH	Tangential	SI (HL, T), SII (HL)

BDA: biotinylated dextran amine; CO: cytochrome-oxidase; SI: primary somatosensory area; SII: secondary somatosensory area; PR: perirhinal cortex; FL: forelimb; HL: hindlimb; LH: left hemisphere; RH: right hemisphere; T: trunk; IL: lower lip; F: face.

chanical stimuli consisting of simple touches or scratches applied on the body surface with sticks and brushes were used to determine somatosensory-driven responses of small clusters of neurons and explore the somatotopic cortical map in SI. After both stereotaxic and electrophysiological determination of the desired cortical location, a single pressure (n = 6 animals) injection of 0.05 μL of 10% BDA (10 kD, Molecular Probes, Eugene, OR), diluted in 0.1 M phosphate buffer (PB, pH 7.4), was made through a glass capillary (40–50 μm internal tip diameter). Two additional animals received an iontophoretic injection of the same tracer applying positive pulses of 2 μA for 20 ms (pipette tip 40 μm). Animals were allowed to recover with food and water ad libitum in the colony. After 15–30 days they were again anesthetized and placed in the headholder for a new series of multiunit mapping of the contralateral (right) somatosensory areas. Electrolytic lesions were produced by applying negative pulses of 10 μA for 10 seconds. At the end of the experiment animals were perfused through the aorta with warm 0.9% saline solution followed by 4% paraformaldehyde in PB.

Histological procedures and anatomical reconstructions

Both hemispheres of six subjects and the left hemisphere of two other cases were dissected from subcortical structures and flattened overnight in fixative between glass slides to be cut on a vibratome (Pelco 1000, Ted Pella, Redding, CA) into serial, tangential 100-μm-thick sections. In two of the cases the right hemispheres were cut into coronal 200-μm-thick sections (see Table 1). Identification of recording and injection sites was assessed by the location of microelectrode electrolytic lesions. Serial tangential or coronal sections from the hemispheres contralateral to the injection were processed to reveal BDA-labeled callosal axons. All sections were incubated overnight in avidin-biotin complex (ABC, Vector Laboratories, Burlingame, CA, 1:200), and processed for nickel-intensified DAB reaction (Shu et al., 1988). Two of the experimental cases (Cc 10 and Cc 17, Table 1) were also histochemically processed for cytochrome oxidase (CO) according to the method of Wong-Riley (1979) in addition to BDA. In these cases electrophysiological mapping could be correlated with the architectonic boundaries in tangential sections. Finally, sections were mounted on gelatinized slides, dehydrated, cleared, and coverslipped with Entellan (Merck, Darmstadt, Germany). In experimental cases Cc 02 and Cc 04, the brains were cut parallel to the coronal plane. In order to reveal cortical lamination, some sections of these animals were counterstained with cresyl violet. Bidimensional reconstruction of the flattened hemispheres was achieved using a camera lucida by matching anatomical landmarks across serial superimposed sections. Thus, the precise cortical location of each injection site in the fore- or hindlimb representation of the left SI area could be compared and correlated with anatomically and functionally determined regions of the right hemisphere, where labeled interhemispheric axons terminate. Table 1 summarizes the experimental cases and axon terminals analyzed in the present work.

For three-dimensional (3D) reconstruction, each axon terminal was digitized directly from the sections using a 60× oil immersion objective on a Optiphot-2 (Nikon, Japan) microscope equipped with a motorized stage (MAC200, LUDL, Hawthorne, NY) and coupled to a computer running Neurolucida software (MicroBrightField, Colchester, VT), thereby allowing for x, y, and z coordinates of digitized points to be stored and analyzed. For the purpose of the present investigation, a digitized axon terminal corresponds to an entire segment with its branches included in one tangential section (100 μm thick). For quantitative analysis, we chose axon terminals that presented, as much as possible, real true ends within a single section. Smaller trees presenting thicker cut ends were not included in the sample.

Sixty-nine callosal axon terminals (35 at the hindlimb and 34 at the forelimb representation) of the homotopic projection, located mainly within layers II and III, but also extending to layer V and VI, were analyzed by Neuroexplorer software (MicroBrightField). A number of morphometric features were measured, including densities of branching points, segments, and boutons per millimeter of axon length. Average densities were computed by dividing the total number of appendages (branching points, segments, or boutons) by the total axon length, obtained by the sum of all intermediate segment lengths. Planar branching angle (in degrees) was measured between each pair of segments at all branching points, in the plane defined by the two rays drawn from the beginning of a branch to its next node or ending. The surface area of an axon terminal was calculated on the basis of the diameters that were assigned to different parts of the processes while tracing them. These calculations treat each process segment as right frustum. Surface Area = (Pi * (R1 + R2) * sqrt (R1 – R2) * (R1 – R2) + (L * L). R1 is radius at the start of line segment, R2 is radius at end of line segment, L is length of line segment (MicroBrightField). Most of the parameters used to measure the morphometric features

were expressed in density values (number of the occurrences of each morphometric feature per fragment divided by the total length of the fragment). Therefore, the results in each case were not affected by the terminal size or by its incomplete labeling and visualization (Amorim and Picanço Diniz, 1996; Gomes-Leal et al., 2002).

Statistical analysis

Statistical analysis followed similar procedures described elsewhere (Steele and Weller, 1995; Schweitzer and Renehan, 1997; Gomes-Leal et al., 2002). We first investigated the presence of features shared by eventual terminal groups in our sample by submitting all of the following quantitative variables to an initial cluster analysis: densities of branches, of segments, of boutons en passant, of boutons terminaux, segment length, terminal area, planar angle of bifurcations, and limb cortical representation from where axon terminals were drawn. The axon classes suggested by such cluster analysis were further assessed by a forward stepwise discriminant function analysis using the software Statistica 6.0 (Statsoft, Tulsa, OK), in order to determine which variables discriminate between two or more naturally occurring groups. This procedure determines whether groups differ with regard to the mean of a variable, and then to use that variable to predict group membership, thereby revealing which variables provided the best separation of classes suggested by cluster analysis. In addition, arithmetic mean and standard deviation were calculated for the variables chosen as best predictors for groups. In all cases, 10 to 12 terminals from each subject were the object of multiple measurements using a dedicated software (Neuroexplorer, MicroBrightField) to process data obtained with Neurolucida. On rare occasions outliers were detected and excluded from all samples based on standard deviations using standard statistical test to detect extreme values in the sample (Ayres, 2005). Parametric statistical analysis was done and two-tailed Student's *t*-tests for two related samples were applied for comparison between axonal groups suggested by multivariate data analysis. Statistical significance was accepted at the 95% confidence level ($P < 0.05$).

Photomicrographics and image processing

Photomicrography was done with a digital camera (Coolpix 950) attached to a Nikon microscope (Mod Optiphot-2). Brightness and contrast of the pictures were adjusted with Adobe Photoshop (Sand Jose, CA) cs2 software.

RESULTS

Injection sites and patterns of contralateral labeling

Figure 1 illustrates an injection site of BDA in the SI representation of the agouti hindlimb. All injection sites exhibited a dense black central core, varying from 0.4–2.5 mm, surrounded by a thinner dark brown halo, where individual cell bodies and axonal segments appeared well defined. In general there was a straight correlation between the injection site core and extent of the contralateral labeling.

Injection sites were always restricted to the forelimb or the hindlimb representation, and yielded conspicuous anterograde labeling of axonal fragments in both hemispheres. In the hemisphere contralateral to the injection, multiple labeled sites were usually observed, with dense terminal labeling in the corresponding limb representations of SI and SII, and heterotopic fields in other areas and/or body parts representations (see below). As shown in Figure 2, the correspondence of body representation sectors between the injection site and the contralateral labeling was ascertained by electrophysiological recording and cytochrome oxidase stain (Dias et al., 2003). For the same volume of injected BDA, a higher intensity of homotopic interhemispheric labeling was found in the forelimb (FL) than in the hindlimb (HL) representation.

Heterotopic interhemispheric SI projections were found both after HL and FL injections. After FL injections, labeled axon terminals were present in both inferior lip and face representations as well as in other cortical areas, such as SII and perirhinal cortex. However, after HL injections labeled axon terminals were present in trunk representations and in SII.

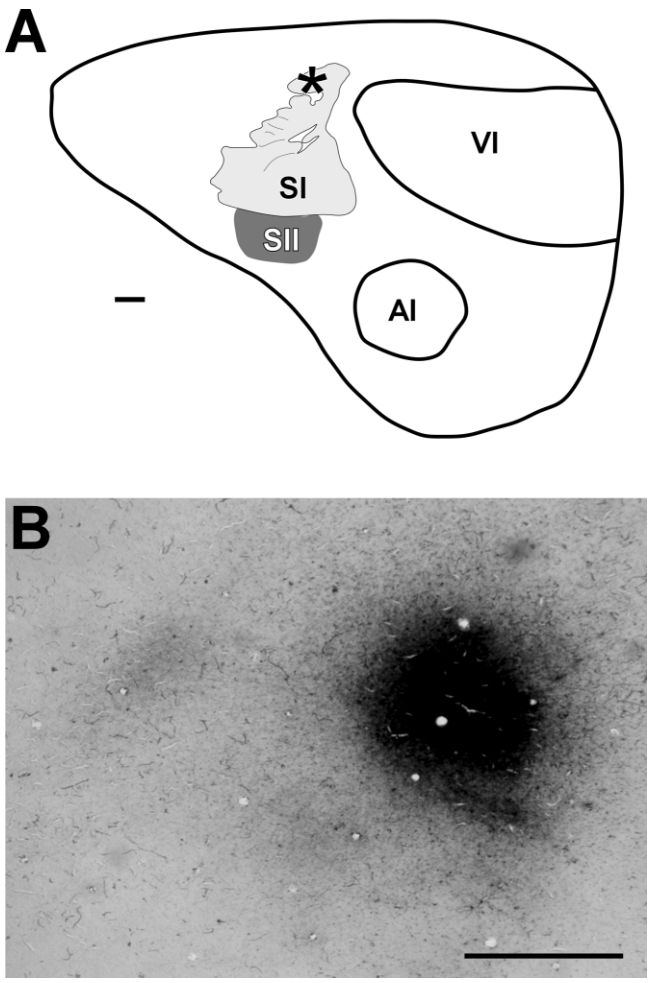

Fig. 1. Schematic picture of case Cc 17 (see also Table 1) showing the position of the injection site in SI (asterisk). Other sensory areas like SII, AI, and VI are also depicted after cytochrome-oxidase histochemistry (**A**). Photomicrography of the tracer injection illustrated in A, localized at the hindlimb representation of agouti's SI (**B**). Scale bar = 1 mm.

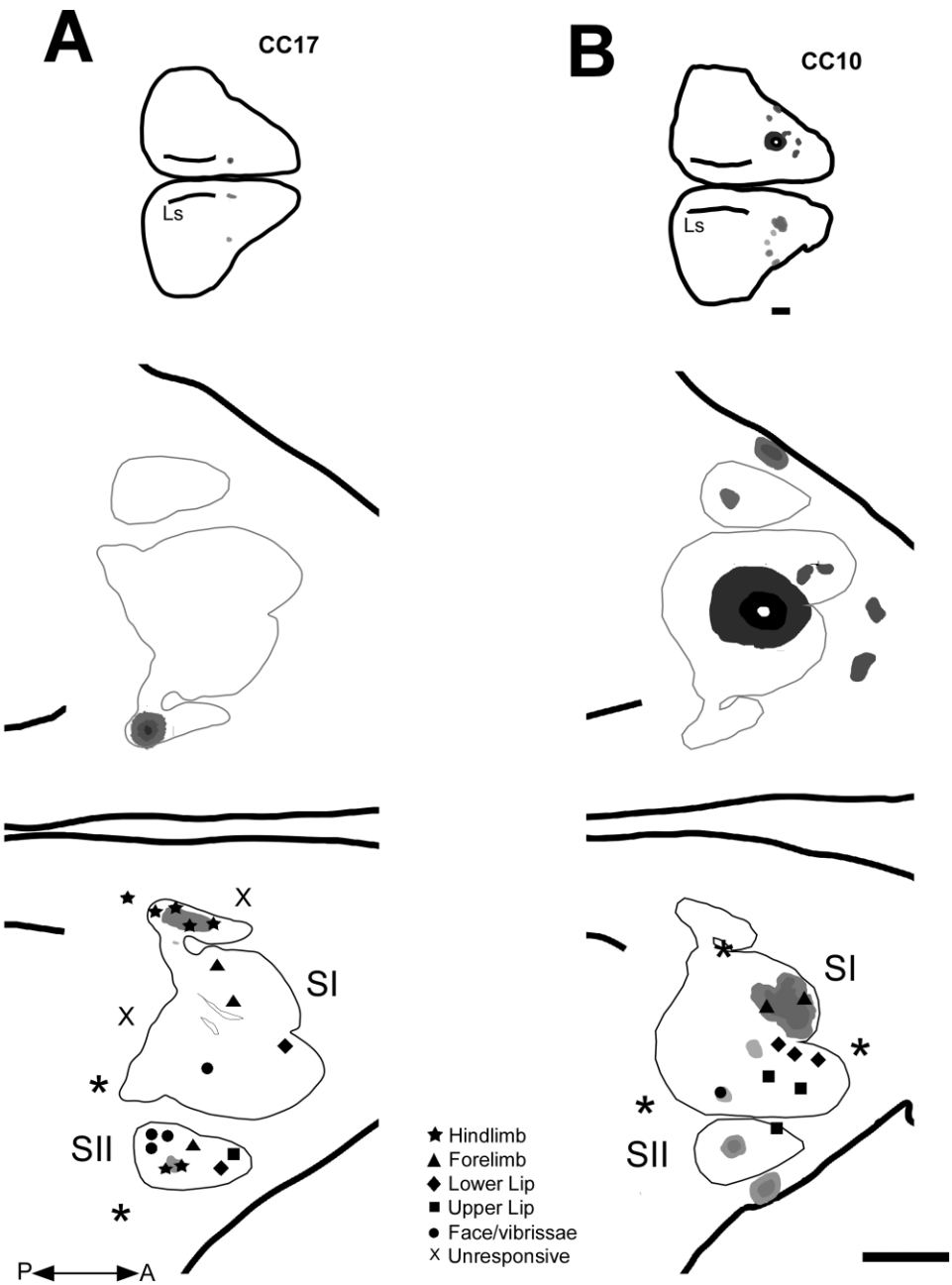

Fig. 2. Tangential reconstructions of ipsi (top) and the contralateral (bottom) labeled hemispheres of case Cc 17 (**A**), in which injections were done into the hindlimb representation. Similar reconstructions for case Cc 10 (**B**), in which injections were done into the forelimb representation. Injection sites (dark and gray areas in top drawing) are indicated on the ipsilateral hemisphere surface, and recording sites (symbols), BDA-labeled regions (light gray areas), and electrolytic lesions (*) are indicated on the contralateral hemisphere (bottom drawings). Thick lines: contours of the tangential section. Thin continuous lines: contours of SI area, as indicated by the envelope of CO-dense regions on alternate section of the right hemisphere, where electrophysiological mapping was performed. Note the match between functionally and anatomically defined areal boundaries. For the drawing of the left (injected) hemisphere, where recording was limited to the injection site, the CO-contours from the right hemisphere were mirror-imaged and superimposed (thin gray lines) to give an approximation of the cortical territories in the ipsilateral side. LS, lateral sulcus; A, anterior; P, posterior. Scale bars = 5 mm; 1 mm (enlargements).

Most labeled structures in the contralateral hemisphere were anterogradely labeled axons, but some scattered retrogradely labeled cell bodies were also found (see Discussion). Interhemispheric axonal fragments both in the FL and in the HL areas were mainly distributed orthogonal or parallel to the pial surface. In all experimental cases contralateral axonal terminals were distributed throughout the cortical depth, mainly in layers II and III, but also extended to layer V and VI.

General morphology and multivariate analysis of callosal axons in the forelimb and hindlimb representations

Qualitatively, significant differences could be devised for FL and HL axons. FL axons (Fig. 3A) are more branched and the parental segment gives rise to shorter and more compact secondary branches than HL axons (Fig. 3B). Figure 3C,D correspond to a sample of the Neurolucida drawings of Type II and Type I axonal fragments. The latter run over longer cortical distances compared with FL axon terminals. Except for the very thick parental segment, axonal branch thickness was similar between terminals found in FL and HL regions of SI. Both FL and HL axons presented boutons terminaux and boutons en passant, and statistical analysis revealed quantitative differences in their respective numbers (see below).

Morphometry and multivariate analyses of FL and HL axons

In order to avoid bias in our interpretation of callosal axonal morphology, we submitted the variables from the axon sample to a cluster analysis followed by a discriminant analysis. Figure 4 displays the dendrogram resulting from cluster analysis performed on the data for 69 SI callosal axon terminals (Arabic numbers in the x axis). This multivariate analysis suggested mainly two classes of axons in the sample, termed I and II.

Discriminant analysis indicated three major variables contributing to discrimination between the groups suggested by cluster analysis (Table 2). These morphometric parameters were axonal field area, density of boutons terminaux, and of branching points. Type II axons present higher axonal field area and densities of branching points and of boutons terminaux than Type I axons (Table 3, Fig. 5; $P < 0.05$). Both axonal types present similar density of en passant boutons (Fig. 5, $P > 0.05$). The variables "density of segments/mm" and "average segment length (μm)" do not contribute to group formation according to discriminant analysis (Fig. 5; $P > 0.05$). Nevertheless, when we compared HL and FL axon terminals without segregation of axon types, we found significant differences for all morphometric features except for branching angle (Fig. 5). 67.56% of the Type II fragments was detected in the FL representation, whereas Type I axon terminals were mainly found in the HL representation (71.87%).

DISCUSSION

The aim of the present study was to compare the morphology of callosal axon terminals that project to the HL and FL representations of SI of the agouti. Cluster analysis of the axonal fragments suggested that there are two axon types, termed Types I and II. A discriminant analysis suggested that these presumptive groups can be separated on the basis of their axonal field area, density of boutons terminaux/mm, and branching points/mm. Statistical comparisons have shown the applicability of this multivariate approach, by which axons that project to both FL and HL representations of agouti SI can be separated from each other. Moreover, it was possible to correlate HL axons to Type I axons and FL axons to Type II axons.

Callosal connections of agouti SI: comparisons with other mammalian species

The morphometric properties of callosal connections in the agouti brain have not been described before. The demonstration that these interhemispheric connections target the representation of the distal extremities in SI is in opposition to some previous descriptions in other species, such as raccoon (Herron and Johnson, 1987), cat (Ebner and Myers, 1965; Jones, 1967; Jones and Powell, 1968), monkey (Pandya and Vignolo, 1968; Jones and Powell, 1969), and rat (Akers and Killackey, 1978; Killackey et al., 1983; Olavarria et al., 1984; Hayama and Ogawa, 1997). These previous reports suggest that only medial regions of the body are interconnected through the corpus callosum. However, our results confirm and expand other studies in monkeys (Killackey et al., 1983), tree shrews (Cusick et al., 1985), rats (Hayama and Ogawa, 1997), rabbits (Ledoux et al., 1987), and raccoons (Guillemot et al., 1992), which described callosal connections in regions of limb representation. In most of these species, callosal connections were described as sparse in the limb representation; however, the rabbit callosal connections described by Ledoux et al. (1987), using electrophysiological recordings and horseradish peroxidase tracing, showed intense labeling in the HL and FL representations in all cortical layers, particularly in Layers II and III. These results are similar to the agouti interhemispheric projections as described in the present report. However it is well documented that some species that use the forepaw in sensory and motor tasks do have few callosal connections in primary forepaw cortex: monkey (Killackey et al., 1983), tree shrew (Cusick et al., 1985), rat (Hayama and Ogawa, 1997), raccoon (Guillemot et al., 1992), and star-nosed mole (Catania and Kaas, 2001). For example, in the monkey brain the hand representation of M1 exhibited a modest homotopic callosal projection, as judged by the small number of labeled neurons within the region corresponding to the contralateral injection, but in contrast, the supplementary motor area (SMA) hand representation showed a dense callosal projection to the opposite SMA. After injection of an anterograde tracer (BDA) in the hand representation of M1, only a few small patches of axonal label were found in the corresponding region of M1, as well as in the lateral premotor cortex, and virtually no label was found in the SMA. Injections of the same anterograde tracer in the hand representation of the SMA, however, resulted in dense and widely distributed axonal terminal fields in the opposite SMA, motor areas, while labeled terminals were clearly less dense in M1 (Rouiller et al., 1994). This suggests that highly corticalized species, such as primates, which present bilateral forelimb coordination, have few callosal connections in primary cortex, but many in higher-order cortex. On the other hand, species that also present bilateral forepaw use, but have smaller brains, like the agouti, have many callosal projections constricted at their primary cortices.

Stereotypy and diversity in callosal neurons seem to coexist both in the same and in different regions of the brain in different species. Indeed, Vercelli and Innocenti (1993) after Lucifer yellow intracellular injections in lightly fixed brain slices guided by retrograde fluorescent labeling, have shown no significant differences between dendritic morphometric features of visual callosal neurons of supragranular homotopical projections inside the same

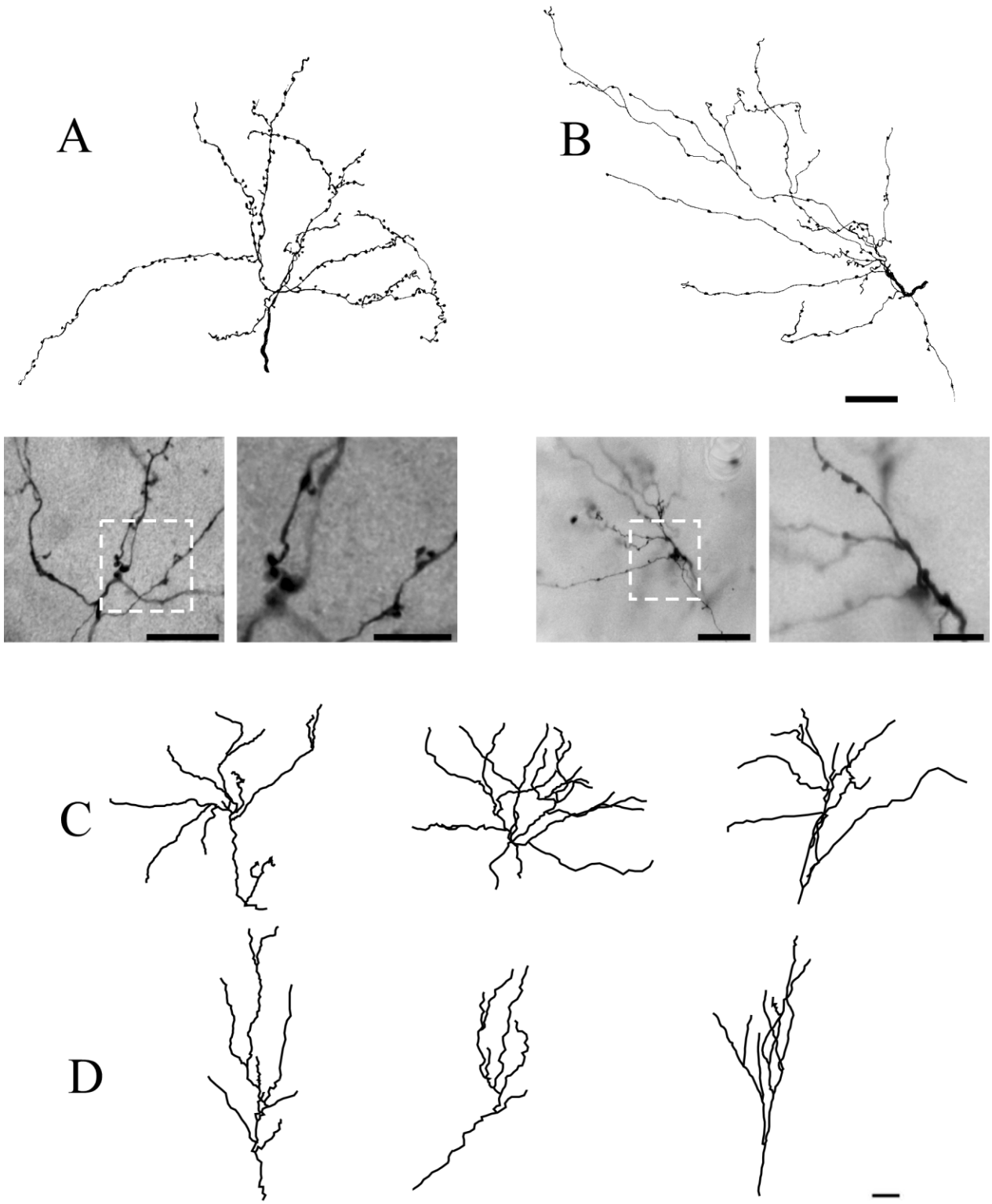

Fig. 3. Photomicrographs and camera lucida drawings of agouti's SI callosal axon arbors. **A,B:** Camera lucida drawings (upper) and photomicrographs (lower) of axon terminals Type II and Type I, respectively (according to cluster analysis), illustrating fine details of the axonal morphology. Dashed white squares on the photomicrographs correspond to high-power photomicrographs in A,B. **C,D:** Graphic representations of Type II and Type I, respectively, camera lucida drawings. A, B scale bar corresponds to: 50 μm; 20 μm and 10 μm respectively. C, D scale bar 50 μm. Scale bars = 50 μm in A,B, 20 μm and 10 μm, respectively; 50 μm in C,D.

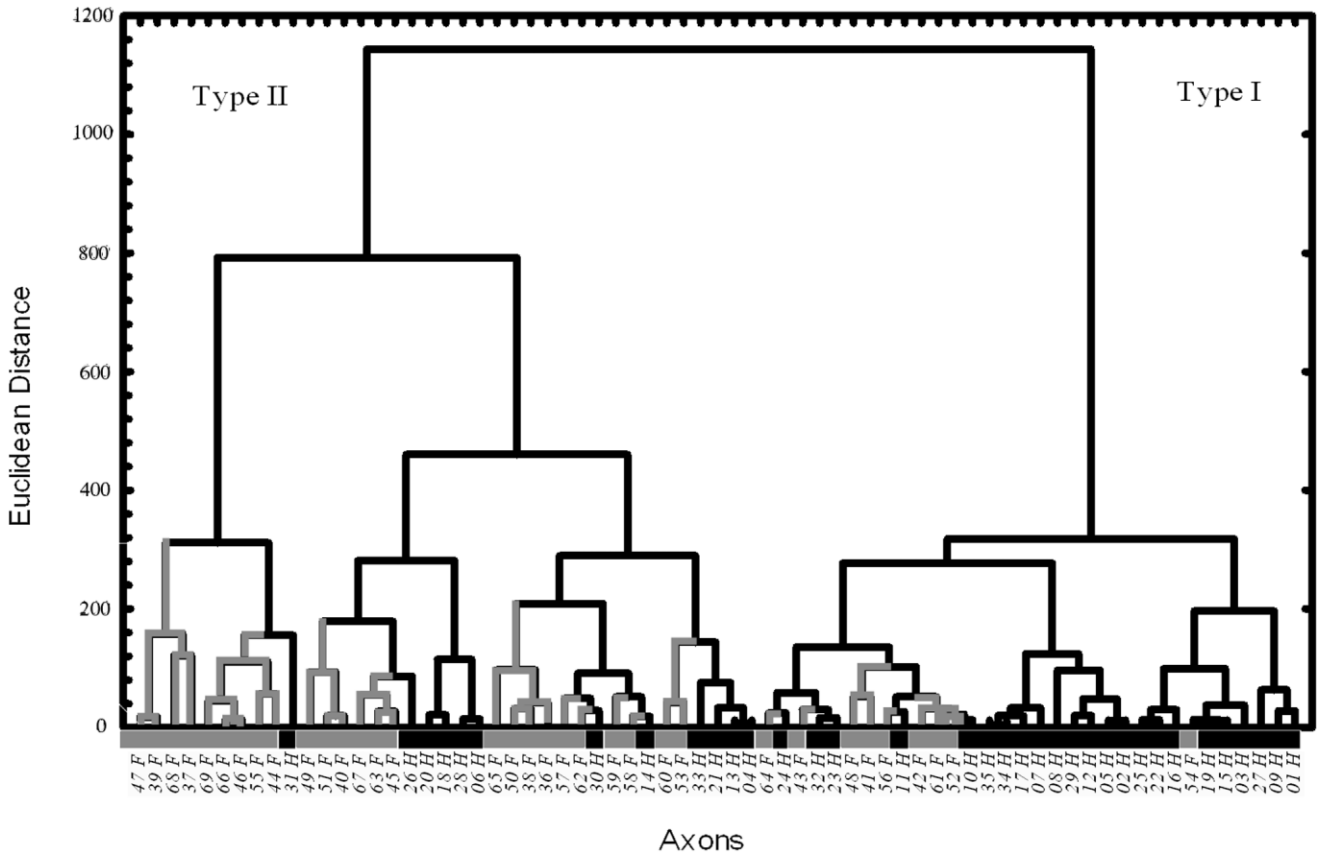

Fig. 4. Dendrogram resulting from cluster analysis performed on the data (Table 2) for 69 SI callosal axon terminals (Arabic numbers). Proposed classes of axons are designated Types I and II. F, forelimb (gray lines); H, hindlimb (black lines).

TABLE 2. Forward Stepwise Discriminant Function Analysis Summary for the Data

Variables	Wilks' lambda	Partial lambda	F-remove	*P*-level	Tolerance
Area	0.949	0.332	130.585	0.000	0.814
Density of branching points	0.354	0.892	7.892	0.006	0.674
Density of boutons terminaux	0.330	0.956	2.950	0.091	0.810

TABLE 3. Morphometric Features of Hindlimb and Forelimb Axon Arbors

Morphometric feature	I	II	*P*	Forelimb	Hindlimb	*P*
Branching points/mm	2.31	3.23	0.01	3.73	2.03	0.00
Boutons en passant/mm	39.85	39.00	0.72	43.00	35.89	0.002
Boutons terminaux/mm	3.59	5.02	0.00	6.50	2.28	0.00
Segments/mm	6.89	6.35	0.43	7.75	5.49	0.001
Segment length (μm)	171.87	173.28	0.93	136.77	207.46	0.00
Terminal field area (μm)	424.76	905.81	0.00	822.87	546.57	0.00

area. However, striking differences have been found between neurons in different areas, and the infragranular neurons exhibited heterogeneous morphologies. In the present report it was described that axonal fragments of homotopical callosal neurons of the agouti somatosensory cortex, inside the same area, present different morphologies in different topographical regions. In both cases (agouti somatosensory and kitten visual projections) stereotypy and diversity were present. It remains an open question how this stereotypy and diversity detected inside and between areas, both at the axonal and dendritic levels, contribute to the callosal physiology.

Additionally, we found a stronger axon labeling in the FL than in HL representation of the agouti, a result that has not been observed in the rabbit (Ledoux et al., 1987). It is possible that that this strong projection to the FL representation in the agouti might be associated with behavioral peculiarities of this species. While forepaws in the rabbit are used predominantly for locomotion, in the agouti they are used both for locomotion and for active tactile examination and manipulation of food. The great representation of the FL in the agouti (Pimentel-Souza et al., 1980) may be related to intermanual coordination, a function that may be associated with the callosal projections (Swinnen, 2002). Since intermanual coordination might require more complex circuits that occupy a larger cortical space, the greater interhemispheric axonal coverage described for the HL might be just a direct consequence of the relative magnification of the forepaw representation. Furthermore, bilateral (hand and food) receptive fields have been described for callosal neurons in

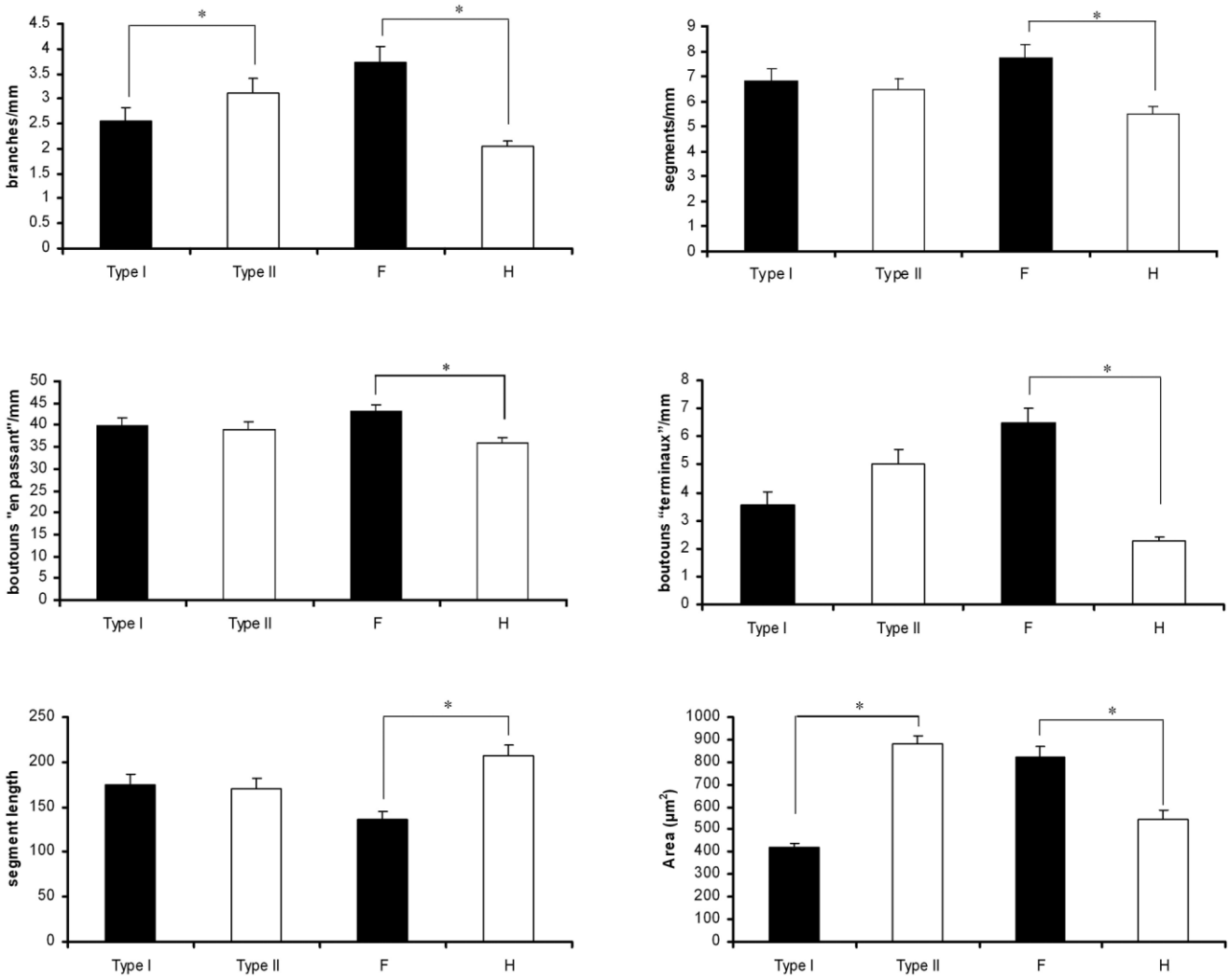

Fig. 5. Density of branching point (**A**), segment density (**B**), boutons en passant (**C**), boutons terminaux (**D**), segment length (**E**), and field area (**F**) of axon arbors of SI somatosensory callosal projections in the agouti. (*$P < 0{,}05$), two-tailed Student's *t*-test. F, forelimb; H, hindlimb.

monkeys (Iwamura et al., 1994; Iwamura and Tanaka, 1996; Taoka et al., 1998), with a higher density of bilateral receptive fields in the hand representation (Iwamura, 2000). These receptive fields were also found in the HL representation of the rat somatosensory cortex (Armstrong-James and George, 1988), which might be related to behavioral tasks that impose HL reciprocal activation.

In humans (Jacobs et al., 2001) and monkeys (Rokni et al., 2003), the coordination of hands and fingers relies on communication through the corpus callosum to an even greater extent than proximal limb movements (Iwamura et al., 2001). This bilateral activity in SI is due to the fact that hands and fingers are controlled mainly by the contralateral hemisphere, whereas the arms can also be controlled to a significant degree by the ipsilateral hemisphere (Brinkman and Kuypers, 1972). The agouti usually sits on its HL, leaving the FL free for food manipulation while eating. This behavior requires intermanual coordination and some kind of interhemispheric integration. We propose that the specialized interhemispheric connections to the FL representation of SI are involved in this intermanual sensory-motor task coordination. The agouti somatosensory cortex is mainly activated by stimulation of the contralateral side of the body (Pimentel-Souza et al., 1980), but ipsilateral or bilateral activation were not systematically investigated in this species and, therefore, this possibility still requires experimental confirmation.

Heterotopic interhemispheric SI projections were found both after HL and FL injections. After FL injections, labeled axon terminals were present in both inferior lip and face representations as well as in other cortical areas, such as SII and perirhinal cortex. The agouti uses the lips and vibrissae to explore food before catching it with the mouth. It manipulates objects using intermanual coordinated movements, together with the lips and mouth, to explore it before deciding to eat or to hide the object. We suggest that heterotopic connections to these SI regions

may be correlated with the integration of these sensorymotor actions.

The observation of callosal projections from SI to SII in the agouti confirm and expand previous studies in other mammals using neurotracers (Pandya and Vignolo, 1968; Jones and Powell, 1969; Herron and Johnson, 1987; Koralek and Killackey, 1990; Krubitzer and Kaas, 1990; Krubitzer et al., 1998; Catania and Kaas, 2001) as well as neuroimage techniques in humans (Disbrow et al., 2000).

Different morphometric patterns of callosal axons of agouti SI

Cluster analysis of our axon sample suggested two major groups of callosal axons projecting to FL and HL representations: Types I and II. Type II axonal terminals present a compact arborization, higher density of branching points and boutons terminaux/mm, and larger axonal field areas than Type I. The latter presents longer and less ramified branches, running over longer cortical distances, but innervating a smaller cortical area. Callosal Type II axons were found mainly in the FL, and Type I in HL representation.

The axonal field area seems to be an important distinctive morphometric feature of axonal pathways in the mammalian cortex. Quantitative multivariate analyses of axons projecting from caudal to rostral inferior temporal cortex of squirrel monkeys revealed the presence of three axonal groups distinguished by their axonal field area, according to discriminant analysis (Steele and Weller, 1995). Type I axons, the smallest in terminal arbor area, were located predominantly within the dorsal rostral inferior (ITC) temporal cortex. Type III axons, largest in areal extent, and Type II axons, intermediate, terminated in the ventral rostral inferior temporal cortex and within a third, transitional region between them (Steele and Weller, 1995). These three classes of axons might correspond to different types of visual information entering rostral inferior temporal cortex (Steele and Weller, 1995). Other studies by our group in cat (Gomes-Leal et al., 2002) and cebus monkey (Amorim and Picanço-Diniz, 1996a,b) striate cortex, using iontophoretic biocytin injections, also demonstrated that intrinsic axons of this cortical region in these mammalian species can be separated in Types I and II on the basis of average segment length and density of axonal boutons, as revealed by cluster and discriminant analyses.

Callosal projections of somatosensory and motor cortices seem to be essential for bimanual interaction. In the agouti, this bilateral sensorimotor behavior is restricted to the forelimbs, which are used in integrated form to manipulate food while eating. In the present study the two classes of agouti's callosal axons might represent morphological specializations related to different modalities of somatosensory information entering the callosal pathways in order to homotopically interconnect those regions of limb and face representation in SI. Callosal axon arbors within the FL representation area are more compact and dense than those in the HL area, in accordance with the predominant role of the former for intermanual coordination related to food intake. It is possible that these circuits represent the neuroanatomical basis of feeding behavior in this species.

Technical considerations

Although rare, unwanted retrograde labeling has been eventually found as a result of large neurotracer injection volumes (King et al., 1989; Chevalier et al., 1992). We detected labeled neuronal cell bodies in the contralateral hemisphere that could be associated with retrograde transport by labeling of fibers of passage. This labeling was more evident in the experimental animals submitted to pressure injections. In both cases (pressure and iontophoretic injections), retrograde labeling has been associated with low, but not with the high molecular weight BDA used in our study (Brandt and Apkarian, 1992; Vercelli and Innocenti, 1993; Reiner et al., 2000; Kobbert et al., 2000). Retrograde labeling with 10 kDa BDA has not been reported extensively, although it is clear that, like other tracers, BDA is taken up by axons that have been damaged by the injection (Brandt and Apkarian, 1992). There is also evidence that BDA can be taken up by intact axon terminals at the injection site (Jiang et al., 1993). This is particularly a concern for large injections, because in this case BDA can be transported both anterogradely and retrogradely and, therefore, labeled afferents cannot be discerned from axons belonging to projection neurons within the same injection site (Deurveilher and Semba, 2005). This cannot be completely excluded in the present investigation, but the protocol used, for example, including a small micropipette inner diameter (~40–50 μm), certainly minimized this possibility.

Although retrograde labeling sometimes occurred even with micropipette injections, retrogradely labeled cells in the contralateral hemisphere were rare and faintly labeled. Considering that this faint retrograde labeling occurred in both FL and HL injection sites, we concluded that this is not a contributor to the differences between the axonal types described in the present report. Transynaptic labeling was not found in previous studies (Brandt and Apkarian, 1992) and no evidence for it was found in the present work.

Finally, 3D anatomical reconstructions of axon terminals from a single thick section assume that part of the axonal tree is located in adjacent sections. Incomplete reconstructions imply that only metric features (for example, density of boutons/mm), which do not depend on the order of the segments, are suitable for analysis. This fact was considered for the morphometric analysis of callosal axons performed in the present study, providing consistent quantitative data that show the same tendencies in each individual group of terminals.

With respect to the histochemical labeling of agouti isocortex, the pattern of CO reactivity often revealed the limits of SI, a result similar to those seen in small rodents using this and other histochemical techniques (Wallace, 1987; Pereira et al., 2000; Freire et al., 2004, 2005). The electrophysiological maps of SI were strictly correlated with the boundaries revealed by CO.

CONCLUSIONS

The study of callosal connections of distal limb portions of S1 of the agouti present data in support of three major conclusions: First, both locations have callosal connections with matching S1 locations in the other hemisphere, as well as in other cortical areas, mainly S2, but also perirhinal cortex. Second, the axon arbors of callosal neurons can

be quantitatively classified into two types, differing in arbor type, branching, and synaptic density. Third, since our data showing that FL axon terminals present great similarity (but not always), and different morphology when compared to the HL axon terminals, it is reasonable to suppose that there is both stereotypy and diversity in the organization of callosal connections.

LITERATURE CITED

Akers RM, Killackey HP. 1978. Organization of corticocortical connections in the parietal cortex of the rat. J Comp Neurol 181:513–537.

Amorim AK, Picanço-Diniz CW. 1996a. Intrinsic projections of cebus-monkey area 17: cell morphology and axon terminals. Rev Bras Biol 56(Su 1 Pt 2):209–219.

Amorim AK, Picanço-Diniz CW. 1996b. Morphometric analysis of intrinsic axon terminals of cebus monkey area 17. Braz J Med Biol Res 29:1363–1368.

Armstrong-James M, George MJ. 1988. Bilateral receptive fields of cells in rat Sm1 cortex. Exp Brain Res 70:155–165.

Ayres M, Ayres M Jr, Ayres DL, dos Santos AS. 2005. Bioestat 4.0 Aplicações Estatísticas nas Áreas das Ciênicas Biológicas e Médicas. 324.

Binzegger T, Douglas RJ, Martin KA. 2005. Axons in cat visual cortex are topologically self-similar. Cereb Cortex 15:152–165.

Brandt HM, Apkarian AV. 1992. Biotin-dextran: a sensitive anterograde tracer for neuroanatomic studies in rat and monkey. J Neurosci Methods 45:35–40.

Brinkman J, Kuypers HG. 1972. Splitbrain monkeys: cerebral control of ipsilateral and contralateral arm, hand, and finger movements. Science 176:536–539.

Cardoso de Oliveira S, Gribova A, Donchin O, Bergman H, Vaadia E. 2001. Neural interactions between motor cortical hemispheres during bimanual and unimanual arm movements. Eur J Neurosci 14:1881–1896.

Catania KC, Kaas JH. 2001. Areal and callosal connections in the somatosensory cortex of the star-nosed mole. Somatosens Mot Res 18:303–311.

Chevalier G, Deniau JM, Menetrey A. 1992. Evidence that biocytin is taken up by axons. Neurosci Lett 140:197–199.

Cusick CG, MacAvoy MG, Kaas JH. 1985. Interhemispheric connections of cortical sensory areas in tree shrews. J Comp Neurol 235:111–128.

DeFelipe J, Elston GN, Fujita I, Fuster J, Harrison KH, Hof PR, Kawaguchi Y, Martin KA, Rockland KS, Thomson AM, Wang SS, White EL, Yuste R. 2002. Neocortical circuits: evolutionary aspects and specificity versus non-specificity of synaptic connections. Remarks, main conclusions and general comments and discussion. J Neurocytol 31:387–416.

Deurveilher S, Semba K. 2005. Indirect projections from the suprachiasmatic nucleus to major arousal-promoting cell groups in rat: implications for the circadian control of behavioural state. Neuroscience 130: 165–183.

Diao YC, So KF. 1991. Dendritic morphology of visual callosal neurons in the golden hamster. Brain Behav Evol 37:1–9.

Disbrow E, Roberts T, Krubitzer L. 2000. Somatotopic organization of cortical fields in the lateral sulcus of *Homo sapiens:* evidence for SII and PV. J Comp Neurol 418:1–21.

Douglas RJ, Martin KA. 2004. Neuronal circuits of the neocortex. Annu Rev Neurosci 27:419–451.

Ebner FF, Myers RE. 1965. Distribution of corpus callosum and anterior commissure in cat and raccoon. J Comp Neurol 124:353–365.

Elston GN, Rosa MG. 2000. Pyramidal cells, patches, and cortical columns: a comparative study of infragranular neurons in TEO, TE, and the superior temporal polysensory area of the macaque monkey. J Neurosci 20:RC117.

Freire MA, Gomes-Leal W, Carvalho WA, Guimaraes JS, Franca JG, Picanco-Diniz CW, Pereira A Jr. 2004. A morphometric study of the progressive changes on NADPH diaphorase activity in the developing rat's barrel field. Neurosci Res 50:55–66.

Freire MA, Franca JG, Picanco-Diniz CW, Pereira A Jr. 2005. Neuropil reactivity, distribution and morphology of NADPH diaphorase type I neurons in the barrel cortex of the adult mouse. J Chem Neuroanat 30:71–81.

Gomes-Leal W, Silva GJ, Oliveira RB, Picanco-Diniz CW. 2002. Computer-assisted morphometric analysis of intrinsic axon terminals in the supragranular layers of cat striate cortex. Anat Embryol (Berl) 205:291–300.

Guillemot JP, Richer L, Ptito M, Guilbert M, Lepore F. 1992. Somatosensory receptive field properties of corpus callosum fibres in the raccoon. J Comp Neurol 321:124–132.

Hayama T, Ogawa H. 1997. Regional differences of callosal connections in the granular zones of the primary somatosensory cortex in rats. Brain Res Bull 43:341–347.

Herron P, Johnson JI. 1987. Organization of intracortical and commissural connections in somatosensory cortical areas I and II in the raccoon. J Comp Neurol 257:359–371.

Houzel JC, Carvalho ML, Lent R. 2002. Interhemispheric connections between primary visual areas: beyond the midline rule. Braz J Med Biol Res 35:1441–1453.

Hubener M, Bolz J. 1988. Morphology of identified projection neurons in layer 5 of rat visual cortex. Neurosci Lett 94:76–81.

Iwamura Y. 2000. Bilateral receptive field neurons and callosal connections in the somatosensory cortex. Philos Trans R Soc Lond B Biol Sci 355:267–273.

Iwamura Y, Tanaka M. 1996. Representation of reaching and grasping in the monkey postcentral gyrus. Neurosci Lett 214:147–150.

Iwamura Y, Iriki A, Tanaka M. 1994. Bilateral hand representation in the postcentral somatosensory cortex. Nature 369:554–556.

Iwamura Y, Taoka M, Iriki A. 2001. Bilateral activity and callosal connections in the somatosensory cortex. Neuroscientist 7:419–429.

Jacobs B, Schall M, Prather M, Kapler E, Driscoll L, Baca S, Jacobs J, Ford K, Wainwright M, Treml M. 2001. Regional dendritic and spine variation in human cerebral cortex: a quantitative Golgi study. Cereb Cortex 11:558–571.

Jiang X, Johnson RR, Burkhalter A. 1993. Visualization of dendritic morphology of cortical projection neurons by retrograde axonal tracing. J Neurosci Methods 50:45–60.

Jones EG. 1967. Pattern of cortical and thalamic connexions of the somatic sensory cortex. Nature 216:704–705.

Jones EG, Powell TP. 1968. The commissural connexions of the somatic sensory cortex in the cat. J Anat 103:433–455.

Jones EG, Powell TP. 1969. Connexions of the somatic sensory cortex of the rhesus monkey. I. Ipsilateral cortical connexions. Brain 92:477–502.

Kaas JH. 2004. Evolution of somatosensory and motor cortex in primates. Anat Rec A Discov Mol Cell Evol Biol 281:1148–1156.

Killackey HP, Gould HJ 3rd, Cusick CG, Pons TP, Kaas JH. 1983. The relation of corpus callosum connections to architectonic fields and body surface maps in sensorimotor cortex of new and old world monkeys. J Comp Neurol 219:384–419.

King MA, Louis PM, Hunter BE, Walker DW. 1989. Biocytin: a versatile anterograde neuroanatomical tract-tracing alternative. Brain Res 497: 361–367.

Kobbert C, Apps R, Bechmann I, Lanciego JL, Mey J, Thanos S. 2000. Current concepts in neuroanatomical tracing. Prog Neurobiol 62:327–351.

Koralek KA, Killackey HP. 1990. Callosal projections in rat somatosensory cortex are altered by early removal of afferent input. Proc Natl Acad Sci U S A 87:1396–1400.

Krubitzer LA, Kaas JH. 1990. The organization and connections of somatosensory cortex in marmosets. J Neurosci 10:952–974.

Krubitzer L, Clarey JC, Tweedale R, Calford MB. 1998. Interhemispheric connections of somatosensory cortex in the flying fox. J Comp Neurol 402:538–559.

Ledoux MS, Whitworth RH Jr, Gould HJ 3rd. 1987. Interhemispheric connections of the somatosensory cortex in the rabbit. J Comp Neurol 258:145–157.

Manger PR, Nakamura H, Valentiniene S, Innocenti GM. 2004. Visual areas in the lateral temporal cortex of the ferret (Mustela putorius). Cereb Cortex 14:676–689.

Migliore M, Shepherd GM. 2005. Opinion: an integrated approach to classifying neuronal phenotypes. Nat Rev Neurosci 6:810–818.

Olavarria JF. 2001. Callosal connections correlate preferentially with ipsilateral cortical domains in cat areas 17 and 18, and with contralateral domains in the 17/18 transition zone. J Comp Neurol 433:441–457.

Olavarria J, Van Sluyters RC, Killackey HP. 1984. Evidence for the complementary organization of callosal and thalamic connections within rat somatosensory cortex. Brain Res 291:364–368.

Pandya DN, Vignolo LA. 1968. Interhemispheric neocortical projections of somatosensory areas I and II in the rhesus monkey. Brain Res 7:300–303.

Pereira A Jr, Freire MA, Bahia CP, Franca JG, Picanco-Diniz CW. 2000.

The barrel field of the adult mouse SmI cortex as revealed by NADPH-diaphorase histochemistry. Neuroreport 11:1889–1892.

Pimentel-Souza F, Cosenza RM, Campos GB, Johnson JI. 1980. Somatic sensory cortical regions of the agouti, Dasyprocta aguti. Brain Behav Evol 17:218–240.

Porter LL, White EL. 1986. Synaptic connections of callosal projection neurons in the vibrissal region of mouse primary motor cortex: an electron microscopic/horseradish peroxidase study. J Comp Neurol 248: 573–587.

Pritzel M, Kretz R, Rager G. 1988. Callosal projections between areas 17 in the adult tree shrew (Tupaia belangeri). Exp Brain Res 72:481–493.

Reiner A, Veenman CL, Medina L, Jiao Y, Del Mar N, Honig MG. 2000. Pathway tracing using biotinylated dextran amines. J Neurosci Methods 103:23–37.

Rokni U, Steinberg O, Vaadia E, Sompolinsky H. 2003. Cortical representation of bimanual movements. J Neurosci 23:11577–11586.

Rouiller EM, Liang F, Babalian A, Moret V, Wiesendanger M. 1994. Cerebellothalamocortical and pallidothalamocortical projections to the primary and supplementary motor cortical areas: a multiple tracing study in macaque monkeys. J Comp Neurol 345:185–213.

Schweitzer L, Renehan WE. 1997. The use of cluster analysis for cell typing. Brain Res Brain Res Protoc 1:100–108.

Shu SY, Ju G, Fan LZ. 1988. The glucose oxidase-DAB-nickel method in peroxidase histochemistry of the nervous system. Neurosci Lett 85: 169–171.

Soloway AS, Pucak ML, Melchitzky DS, Lewis DA. 2002. Dendritic morphology of callosal and ipsilateral projection neurons in monkey prefrontal cortex. Neuroscience 109:461–471.

Steele GE, Weller RE. 1995. Qualitative and quantitative features of axons projecting from caudal to rostral inferior temporal cortex of squirrel monkeys. Vis Neurosci 12:701–722.

Swinnen SP. 2002. Intermanual coordination: from behavioural principles to neural-network interactions. Nat Rev Neurosci 3:348–359.

Taoka M, Toda T, Iwamura Y. 1998. Representation of the midline trunk, bilateral arms, and shoulders in the monkey postcentral somatosensory cortex. Exp Brain Res 123:315–322.

Vercelli A, Innocenti GM. 1993. Morphology of visual callosal neurons with different locations, contralateral targets or patterns of development. Exp Brain Res 94:393–404.

Voigt T, LeVay S, Stamnes MA. 1988. Morphological and immunocytochemical observations on the visual callosal projections in the cat. J Comp Neurol 272:450–460.

Wallace MN. 1987. Histochemical demonstration of sensory maps in the rat and mouse cerebral cortex. Brain Res 418:178–182.

Wong-Riley M. 1979. Columnar cortico-cortical interconnections within the visual system of the squirrel and macaque monkeys. Brain Res 162: 201–217.